(article starts on next page)

Steps and catalytic reactions: CO oxidation with preadsorbed O on Rh(553)☆

Chu Zhang [a], Baochang Wang [b,g], Anders Hellman [b,g], Mikhail Shipilin [c], Andreas Schaefer [f,g], Lindsay R. Merte [d], Sara Blomberg [e], Xueting Wang [f,g], Per-Anders Carlsson [f,g], Edvin Lundgren [a], Jonas Weissenrieder [h], Andrea Resta [i], Anders Mikkelsen [a], Jesper N. Andersen [a], Johan Gustafson [*,a]

[a] *Synchrotron Radiation Research, Lund University, Box 118, 221 00, Lund, Sweden*
[b] *Department of Physics, Chalmers University of Technology, 412 96, Gothenburg, Sweden*
[c] *Department of Physics, AlbaNova University Center, Stockholm University, 106 91, Stockholm, Sweden*
[d] *Material Science and Applied Mathematics, Malmö University, 205 06, Malmö, Sweden*
[e] *Department of Chemical Engineering, Lund University, Box 124, 221 00, Lund, Sweden*
[f] *Department of Chemistry and Chemical Engineering, Chalmers University of Technology, 412 96, Gothenburg, Sweden*
[g] *Competence Centre for Catalysis, Chalmers University of Technology, 412 96, Gothenburg, Sweden*
[h] *Materials and Nano Physics, Department of Applied Physics, KTH Royal Institute of Technology, 100 44, Stockholm, Sweden*
[i] *Synchrotron SOLEIL, L'Orme des Merisiers, 91192, Saint-Aubin, State Two, France*

ARTICLE INFO

ABSTRACT

Industrial catalysts are often comprised of nanoparticles supported on high-surface-area oxides, in order to maximise the catalytically active surface area and thereby utilise the active material better. These nanoparticles expose steps and corners that, due to low coordination to neighboring atoms, are more reactive and, as a consequence, are often assumed to have higher catalytic activity. We have investigated the reaction between CO and preadsorbed O on a stepped Rh(553) surface, and show that CO oxidation indeed occurs faster than on the flat Rh(111) surface at the same temperature. However, we do find that this is not a result of reactions at the step sites but rather at the terrace sites close to the steps, due to in-plane relaxation enabled by the step. This insight can provide ways to optimize the shape of the nanoparticles to further improve the activity of certain reactions.

1. Introduction

An automotive catalytic converter transforms poisonous exhaust gas into comparably less harmful gas. Especially, the three-way catalysts in petrol-driven cars oxidize CO and unburned fuel to CO_2 and H_2O, and simultaneously reduce NO_x to N_2 and O_2 [1–3]. However, understanding these processes on an atomic level is still challenging, especially as it is difficult to study the active surface of a complex industrial catalyst. In order to fill this knowledge gap, single crystals are often studied, under well-controlled conditions, as model systems. These studies are most often performed on flat low-index surfaces, although steps and other defects are believed to govern much of the activity on real catalysts that are based on oxide supported nanoparticles [4–15]. A common approach to study the effect of steps is to use vicinal surfaces with low-index terraces separated by a large number of periodic steps [5,14,16–18].

Atoms along steps have fewer neighbors than atoms on flat surfaces, hence they are assumed to be more reactive. That vicinal surfaces indeed are more reactive has been found in several studies [18–25]. Especially, relevant for CO oxidation over Rh(553), both CO and O are found to adsorb preferentially on steps at low coverages [5,18]. There is, however, a widely spread semantic misconception between reactive (tending to react chemically) and catalytically active (promoting a catalytic reaction). Especially, a too reactive surface will not be catalytically active

---

since the reactants will bind too strongly to react with each other, as described by the Sabatier principle [26].

In this paper, we studied the reaction between CO and preadsorbed O on a stepped Rh(553) with in-situ X-Ray Photoelectron Spectroscopy (XPS) and Density Functional Theory (DFT) coupled with kinetic Monte Carlo (kMC) simulations. We find that the reaction rate is faster on Rh (553) than on flat Rh(111), showing that the stepped surface is indeed more catalytically active. The reaction on the stepped surface Rh(553) happens in sequences and slows down after removing 25% and 50% of the O, and towards the end of the experiment, the O coverage seems to converge towards 25% of the initial coverage. Furthermore, our results show that the reaction occurs on the terraces, while the O atoms bound to the step edges are significantly less prone to react with CO. Hence, the stepped Rh(553) surface is indeed more catalytically active; however it is not the steps that are more active but rather the terraces in the vicinity of the steps.

2. Experimental and computational methods

The measurements were done at the XPS station of beamline i311 at the MAX IV laboratory in Lund, Sweden [27]. The single crystals were cleaned by cycles of Ar^+ sputtering (1.5 kV 20 mA, 20 min at room temperature, 2×10^{-7} mbar) and annealing (950°C for 2 min) followed by oxygen treatment (1×10^{-6} mbar during temperature ramps 250°C - 700°C - 250°C) in order to remove any carbon from the surface. Residual O was removed by flashing the sample to 900°C. The cleanliness of the surfaces was checked by Low Energy Electron Diffraction (LEED) and XPS, which indicated a well ordered structure without any impurities. The surface was exposed to gases by backfilling the chamber.

The spectra were fitted using Doniach-Sunjić lineshapes convoluted with Gaussian lineshapes. A linear background was also subtracted from the spectra. The binding energy scale was calibrated against the Fermi edge. The O 1s spectra were measured with a photon energy of 650 eV, while the C 1s spectra were measured at 360 eV.

The first-principles calculations were performed using density functional theory (DFT) as implemented in the VASP package [28–30]. The interaction between the valance electrons and the core follows the projector augmented wave (PAW) method [31]. PAW potentials with the valence state 2s and 2p for O and C and 4d and 5s for Rh have been employed. A plane wave basis with a kinetic energy cut-off of 400 eV was used. The exchange-correlation (XC) interaction was treated at the level of the generalized-gradient approximation (GGA) using the xc-functional of Perdew, Burke, and Ernzerhof (PBE) [32]. The Rh(111) and Rh(553) surfaces were modeled as slabs with a vacuum region of 20 Å added between the periodic images. The slabs of Rh(111) and Rh (553) were 5 and 15 atomic layers thick, respectively. A $6 \times 6 \times 1$ k-point grid for Rh (111) and $6 \times 3 \times 1$ for Rh (553) were adopted. The atomic positions were optimized until the forces were smaller than 0.03 eV/Å. CO oxidation barriers and diffusion barriers of O atoms migration were calculated via the climbing image nudged elastic-band (CI-NEB) method[33].

All kMC simulations were performed with the *kMCLib* v1.1 software package [34,35]. *kMCLib* is a framework for *lattice* kMC, which allows for arbitrarily complex elementary processes to be included in the simulations. Rates can be given as input before the simulation starts or can be updated on-the-fly during the simulations via a rate calculator interface written in the Python programming language (see SI for details).

The Rh(111) is the close-packed terrace, while the Rh(553) surface consists of 5 atoms wide terraces (including the atoms partly hidden underneath the steps) with monoatomic steps exposing a (111) microfacet. Exposing this surface to 1 L (1 Langmuir = exposure corresponding to 1 s at 1×10^{-6} Torr or 1.3×10^{-6} mbar) of O_2 at liquid nitrogen temperature results in a coverage of 0.4 ML (1 ML = the same number of atoms as in the substrate surface layer, including the atoms partly hidden under the steps) and the detection of a single peak at 529.5 eV in the

O 1s spectrum, as shown in the top left panel of Fig. 1A. The oxygen structure exhibits a (2×1) periodicity on the (111) terraces and a zigzag pattern along the step edges, as shown in Fig. 1B [5]. This yields four different adsorption sites; two on the terraces (denoted O2 and O3), one above (O1), and one below (O4) the step edge. All of these are effectively three-fold hollow sites and indistinguishable in the O 1s spectrum. As expected, the corresponding C 1s spectrum has no peak. This structure is the starting point of the experiment in this paper.

Exposing the clean Rh(553) surface to 0.75 L of CO results in a (2×2)-2CO structure with CO in on-top as well as hollow sites on the (111) terraces [36], as shown in Fig. 1C. Along the steps, the CO molecules initially adsorb in on-top sites but move towards bridge or hollow sites upon increasing coverage [20]. The model shows only CO in bridge sites along the steps for simplicity; however, a low intensity corresponding to CO in on-top sites at steps is found in the C 1s spectra for CO on clean Rh (553) surface.

Fig. 1 D shows the model of the surface after the experiment, where the oxygen atoms on the terraces are removed and replaced by a $(\sqrt{3} \times \sqrt{3})R30°$ structure of CO. The O atoms underneath the steps are, however, still present.

3. Results

3.1. XPS

Fig. 2A and B shows in situ O 1s spectra from the reduction of the oxygen covered Rh(553) surface by CO at room temperature. The CO pressure was initially 1×10^{-9} mbar, but was increased to 1×10^{-8} mbar after an exposure of 0.9 L. Fig. 2A shows how the O coverage is reduced and gives room for CO to adsorb on the surface, but during this experiment, not all O is removed from the surface. Fig. 2B shows selected spectra during the reduction, fitted in order to get information on adsorption sites and coverages. In the O 1s spectrum, we cannot distinguish between CO adsorption on step or terrace, but the CO molecules adsorb almost exclusively in on-top sites.

Fig. 2C shows the development of the different peak areas, expressed as estimated coverage calibrated against a maximum O coverage of 0.4 ML. The most striking feature of this plot is the different reaction rates indicated by the dashed curves. These dashed curves are intended as guides for the eyes only. After the removal of approximately 25% and 50% of the oxygen, the reaction rate drops slightly, and although we did not reach full convergence, the reduction seems to converge towards the removal of 75% of the oxygen. This indicates that the four oxygen sites show different catalytic activity and that one of them is inactive under these conditions.

Looking at the total O coverage, the oxygen coverage is reduced by 50% after a dose of approximately 5 L CO. A similar experiment performed on Rh(111) is shown in the supplementary material, showing that after exposure to 55 L CO, the O coverage is reduced by slightly less than 50%. This shows that, for reaction with the first 50% of the O, the stepped surface is about ten times more active than the flat surface.

In order to get more information about the final structure, we evacuated the chamber, cooled down the sample to liquid nitrogen temperature, and measured detailed O 1s and C 1s spectra as shown in the middle panel of Fig. 1A. As compared to the corresponding spectra from CO adsorbed on the clean Rh(553) surface (bottom of Fig. 1A), the resulting total O 1s signal is slightly more intense in the spectrum with preadsorbed oxygen, due to the coexistence of O and CO on the surface. In contrast, the corresponding C 1s spectrum is clearly lower in intensity, showing that the oxygen is blocking CO adsorption sites. From the fitting of the C 1s spectra, it is clear that significantly less CO is adsorbed on the steps, and what is still adsorbed is found in a different adsorption site (on-top) as compared to when CO was adsorbed on the clean Rh(553) surface (three-fold hollow/bridge). This strongly indicates that the O atoms that are left on the surface are bound to the steps rather than to
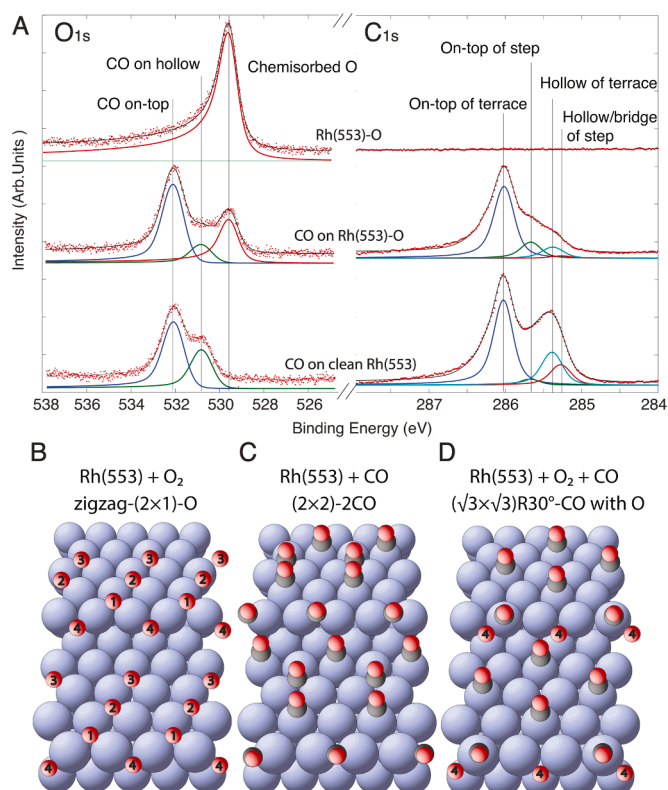
Fig. 1. XPS and models of the Rh(553) surface with adsorbed O and CO.
(A) XPS of the Rh(553) after exposure to O (top), after partial reduction of the chemisorbed O phase by CO (middle), and after exposure of the clean surface to CO (bottom). The chemisorbed O atoms always adsorb in three-fold hollow sites, resulting in a single peak in O 1*s*. In the O 1*s* spectra, we can distinguish between CO molecules in on-top or hollow/bridge sites, but not between CO molecules on the terrace or step. This can instead be done in the C 1*s* spectra. (B) Rh(553) with five atoms wide (111) terraces separated by monoatomic steps with (111) microfacets. Exposure to oxygen results in a (2×1) structure on the terraces and a zigzag structure along the step edges at a saturation coverage of 0.4 ML. (C) CO molecules initially adsorb in on-top sites on both the terraces and the step edges. After saturation with 0.75 L of CO, however, a (2×2)-2CO structure with CO molecules in on-top as well as hollow sites is found on the (111) terraces, while on the steps, CO molecules have shifted toward bridge sites [19,20]. (D) After reducing the O covered surface with CO at room temperature, there is still about 0.1 ML O left. While this does not seem to affect the signals from CO on terraces, CO bound to the steps are, to a larger extent, found in on-top sites rather than hollow or bridge. Hence, the remaining oxygen atoms are found at or close to the steps.

the terraces. Hence, although the stepped surface is more active than the flat one, it seems it is not the steps themselves that are active but rather the flat terraces in the vicinity of the steps.

3.2. Calculations

The adsorption energies of O and CO are determined by the reactivity of the Rh facet. On Rh(111), the calculated O absorption energy at a coverage of 0.25 ML and in a p(2×2) structure is -2.07 eV, while at 0.5 ML and in a p(2×1) structure, it is -2.01 eV. The decrease in adsorption energy is a result of lateral interactions, e.g., sharing of Rh atoms. On the Rh(553) surface, there exist four distinct hcp adsorption sites for oxygen. The first is directly above the step (O1), followed by two terrace sites (O2, O3), and finally, a site directly below the step (O4), see Fig. 1B. For a single O atom, the most favorable site is O1, with an adsorption energy of -2.12 eV, followed by -2.01 eV (O2), -1.97 eV (O3) and -1.79 eV (O4). There is, however, a co-adsorption effect on the step sites that results in

stronger binding of -2.36 eV and -1.94 eV for O1 and O4, respectively, if the other site is also occupied. All adsorption energies of oxygen are presented in Table S1 in the supplementary material.

In the case of CO, four different sites are studied on both facets. According to the calculations, the stable adsorption site for CO on Rh (111) is the hcp site, while bridge/top site(s) is the most stable one(s) on Rh(553). The experimentally observed stable adsorption sites for CO on Rh(111) are on-top and hollow sites, which is different as compared to the DFT results. The difference can be attributed to the drawbacks of the used XC functional [37]. However, as adsorption sites do not significantly affect the relative values of reaction barriers for CO oxidation, the DFT results can still be used to study the reaction qualitatively. The adsorption energies of CO is slightly larger on Rh(553) than on Rh(111), -1.96 eV and -2.05/-2.04 eV, respectively. All adsorption energies for CO are shown in Table S2, and our values agree well with what is reported in the literature [20,38].

Fig. 3 A shows the calculated reaction barriers controlling the CO oxidation for Rh(111), as well as, Rh(553). On the p(2×1) structure of adsorbed oxygen on Rh(111), the barriers were calculated to be 0.96 eV and 0.90 eV for removal of the first and second O atom, respectively. On Rh(553), the picture becomes much more complex, owing to the existence of four distinct O adsorption sites. Here the lowest barrier for removal of the first oxygen was calculated to be only 0.74 eV and was found for the O2 site. The lowest barrier for direct removal of the second oxygen (on site O3) was calculated to be 1.04 eV. However, a lower barrier of 0.78 eV was found for oxygen in O3 via diffusion to the O2 site (the diffusion barrier between site O3 and O2 is only 0.47 eV).

This indicates that the removal of oxygen from both O2 and O3 is expected to be fast as compared to the (111) surface. The third oxygen (situated in O1) also diffuses (barrier of 0.81 eV) to O2 before performing CO oxidation with a barrier of 0.93 eV, which is similar in height to what was calculated for the (111) surface. Finally, the fourth oxygen atom (O4) diffuses away from the step, with a barrier of 1.13 eV before it reacts with CO with a barrier of 1.18 eV. Both these barriers are significantly higher than the ones found for Rh(111).

The differences in reaction barriers directly explain the experimental results, with half of the O atoms being removed more easily than on Rh (111) (with a change in reaction rate after 25%), the next 25% being removed with a speed comparable to Rh(111) and the final 25% not being removed within the time frame of this experiment.

For further analysis, a kMC model was set up based on the reaction landscape obtained from DFT calculations. All elementary processes, together with the barrier values, included in the kMC model are shown in Table S3. The kMC results of O coverage vs time at T = 298.15 K are shown in Fig. 3 (B-C). It is clearly seen that the removal of O from the surface displays three distinct regions. The first 25% of the O atoms are removed very quickly (within 2 s) from the O2 sites. When this process is complete, these sites are refilled by diffusion from O3 (faster), as well as, from O1 (slower) sites as seen by the increased coverage. Especially the removal of atoms from O3 sites, via O2, is still reasonably fast, and after about 200 s, 50% of the O is removed. From here, however, the reaction rate slows down significantly, and it takes about 5000 s before the O atoms originating in O1 sites are removed (Fig. 3 (C)). Finally, the O atoms from the step bottom sites (O4) take no part in the CO oxidation reaction at the simulation temperature. Although the reaction rates do not match perfectly, the general behavior is in good agreement with the experiments and confirms the interpretation of the reaction process.

4. Discussion

Our results show that the reaction between CO and preadsorbed O happens faster on the stepped Rh(553) surface than on the flat Rh(111) surface. This agrees with the general assumption that surfaces with under-coordinated step atoms, since these are more reactive, are more catalytically active. At a closer look, however, this is rather surprising since higher reactivity means that the reactants are bound more strongly

A

B

C
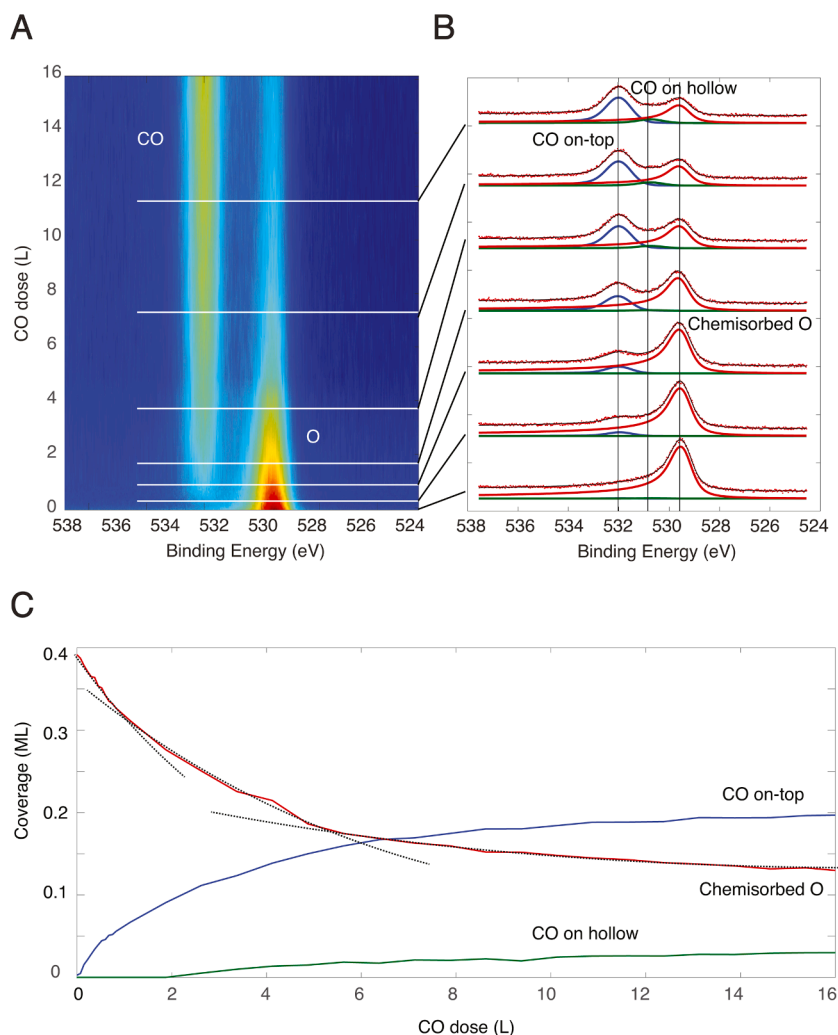
Fig. 2. *In situ* **XPS O 1s spectra during the reduction of Rh (553)-O structure by CO at room temperature.** The CO pressure was 1×10^{-9} mbar until a dose of 0.9 L, then increased to 1×10^{-8} mbar. (A) The live measurement as a 2D plot. (B) The selected spectra decomposed in order to follow the reduction process. (C) the development of the different components, extracted from fitting all the spectra in (A). The dashed curves indicate the three regimes of reduction speed from 0.4 to 0.3, 0.3 to 0.2, and 0.2 to 0.1 ML, respectively. The last 0.1 ML of O is not removed within the time of the experiment under the present conditions. The coverage is estimated by assuming an initial coverage of 0.4 ML (see Fig. 1A). In O 1s we cannot distinguish between CO on terraces or steps.

to the surface, which should make the reaction more difficult. Indeed, our results show that the reaction does not occur on the steps but rather on the terraces in the vicinity of the steps.

Similar studies have previously been performed on vicinal Pt surfaces [39–42]. The general behavior is found to be similar, with both CO and O preferentially adsorbing on the step and a higher activity on the stepped surfaces. In contrast to the present results, the studies of Pt identified two different active sites, corresponding to O2, on the terrace as in this study, and O4 underneath the step. This difference is most likely explained by the type of step investigated; the Rh(553) surface with so-called B-type steps hosts O4 in a three-fold-hollow site, whereas the reported (533), (211), and (311) surfaces of Pt expose A-type steps with O4 being in four-fold-hollow sites. O generally prefers three-fold-hollow sites and is consequently more strongly bound and more difficult to remove in the O4 sites on Rh(553). The model of A and B-type steps are demonstrated in the supplementary material.

A recent study of CO oxidation over a curved Pd crystal under realistic conditions shows, in analogy with our results, that the reaction starts at a lower temperature on the stepped parts of the surface than on the flat (111) facet [43]. Due to the broken bonds, surface atoms generally want to be closer together than atoms in the bulk. Unless there is a surface reconstruction, however, the only distances that may change are the out-of-plane distances, while the in-plane distances between surface atoms, as well as adsorbates, are unchanged. Near a step, the atoms may also contract in the surface plane, resulting in adsorption

sites being closer together. This in turn leads to lower adsorption energy for CO, which hence desorbs, allowing oxygen to adsorb and start the reaction, at a lower temperature.

Hence, CO starts to desorb at a lower temperature on the stepped surfaces, allowing oxygen to adsorb and start the reaction.

In the case of Rh(553), there are in-plane contractions ranging between 0.3% to 1.8%, which further stress the importance of steps in heterogeneous catalysis, although in the case of CO oxidation on Rh (553) not to introduce uncoordinated sites but instead to release strain in the accompanying terrace. As a consequence, some of (553) terrace sites are more catalytic active as compared to the (111) terrace sites.

Our results also emphasize the role of diffusion in the catalytic reaction. Although only one of the O adsorption sites on Rh(553) has a lower reaction barrier than Rh(111), the reaction is significantly faster all the way to the removal of 50% of the O. This indicates that the number of active sites may not be as important as one would think, if there is a possibility for reactants in nearby adsorption sites to diffuse to the active site. This is especially so since highly active sites are occupied for very short times before the reaction occurs, and the site is vacated again. This is supported by recent studies of CO oxidation over Pt(111) and Pt(322), showing three different reaction paths; one for the flat (111) terraces, one direct path at the step and one including diffusion to the step [44,45]. These studies also conclude that, at relatively low temperatures, the steps dominate the reaction through the diffusion pathway.
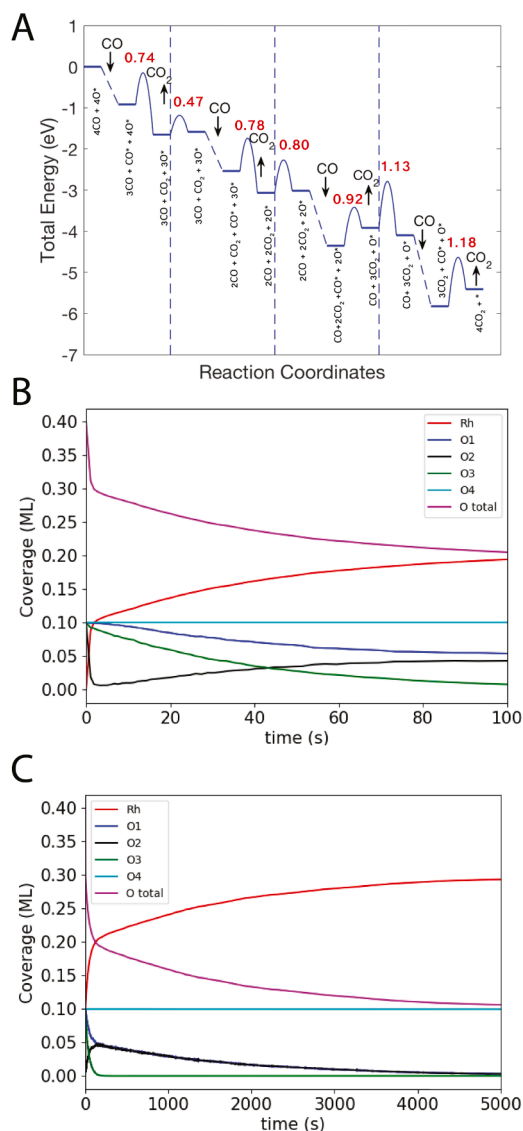
Fig. 3. Combined DFT and kMC simulation of the reduction of the chemisorbed oxygen phase on Rh(553). (A) DFT calculated reaction energy landscapes on the stepped Rh(553) surface. The dashed curves separate different regions corresponding to removing different O atoms from the surface. (B) kMC simulation results of O coverage vs. time on Rh(553) at T = 298.15 K in the first 100 s. The coverage evolution with time of total surface O atoms, O atoms at different surface sites, and bare surface sites is plotted in the same figure. (C) Changes in coverage of the individual species over a period of 5000 s.

5. Conclusions

We have found that the reaction between CO and preadsorbed O proceeds faster on a stepped Rh(553) surface than on flat Rh(111), indicating that the stepped surface is more catalytically active than the flat one. In contrast to what one might assume, however, the reaction does not occur on the step edges but the terraces. These results stress a common misconception that higher reactivity of under-coordinated atoms automatically leads to higher catalytic activity, while, due to a stronger bond to the surface, it actually might lead to lower activity. In addition, however, the step allows for in-plane relaxation of the atomic structure on the terrace, which in turn lowers the reaction barriers on the terraces in the vicinity of the steps. We also find that the number of active sites is not as crucial as one might first expect if reactants can diffuse from nearby adsorption sites to the active sites. This insight can provide ways to optimize the shape of catalytic nanoparticles to further improve the activity of certain reactions.

CRediT authorship contribution statement

Chu Zhang: Investigation, Formal analysis, Visualization, Writing – original draft. **Baochang Wang:** Investigation, Formal analysis, Visualization, Writing – review & editing. **Anders Hellman:** Investigation, Formal analysis, Supervision, Visualization, Writing – review & editing. **Mikhail Shipilin:** Investigation. **Andreas Schaefer:** Investigation, Writing – review & editing. **Lindsay R. Merte:** Investigation, Writing – review & editing. **Sara Blomberg:** Investigation. **Xueting Wang:** Investigation. **Per-Anders Carlsson:** Investigation. **Edvin Lundgren:** Investigation. **Jonas Weissenrieder:** Investigation. **Andrea Resta:** Investigation. **Anders Mikkelsen:** Investigation. **Jesper N. Andersen:** Investigation. **Johan Gustafson:** Project administration, Supervision, Investigation, Formal analysis, Visualization, Writing – review & editing.

Declaration of Competing Interest

The authors declare that they have no known competing financial interests or personal relationships that could have appeared to influence the work reported in this paper.

Acknowledgement

Supplementary materials

Supplementary data associated with this article can be found, in the online version, at doi:10.1016/j.susc.2021.121928.

References

[1] R. Imbihl, G. Ertl, Oscillatory kinetics in heterogeneous catalysis, Chem. Rev. 95 (1995) 697–733, https://doi.org/10.1021/cr00035a012.

[2] A.T. Bell, The impact of nanoscience on heterogeneous catalysis, Science 299 (5613) (2003) 1688–1691.

[3] H. Gandhi, G. Graham, R. McCabe, Automotive exhaust catalysis, J Catal 216 (1) (2003) 433–442, https://doi.org/10.1016/S0021-9517(02)00067-2.40th Anniversary Commemorative Issue

[4] S. Blomberg, R. Westerström, N.M. Martin, E. Lundgren, J.N. Andersen, M. E. Messing, J. Gustafson, A high pressure x-ray photoelectron spectroscopy study of oxidation and reduction of rh(100) and rh nanoparticles, Surf. Sci. 628 (2014) 153–158.

[5] J. Gustafson, A. Resta, A. Mikkelsen, R. Westerström, J.N. Andersen, E. Lundgren, J. Weissenrieder, M. Schmid, P. Varga, N. Kasper, Oxygen-induced step bunching and faceting of rh(553): experiment and ab initio calculations, Phys. Rev. B 74 (3) (2006) 035401.

[6] A.J. Jaworowski, A. Beutler, F. Strisland, R. Nyholm, B. Setlik, D. Heskett, J. N. Andersen, Adsorption sites in o and co coadsorption phases on rh(111) investigated by high-resolution core-level photoemission, Surf. Sci. 431 (1) (1999) 33–41.

[7] L.H. Dubois, G.A. Somorjai, The chemisorption of co and co$_2$ on rh(111) studied by high resolution electron energy loss spectroscopy, Surf. Sci. 91 (2–3) (1980) 514–532.

[8] S. Schwegmann, H. Over, V. De Renzi, G. Ertl, The atomic geometry of the o and co +o phases on rh(111), Surf. Sci. 375 (1) (1997) 91–106.

[9] J. Schoiswohl, S. Eck, M.G. Ramsey, J.N. Andersen, S. Surnev, F.P. Netzer, Vanadium oxide nanostructures on rh(111): promotion effect of co adsorption and oxidation, Surf. Sci. 580 (1) (2005) 122–136.

[10] M. Gierer, A. Barbieri, M.A. Van Hove, G.A. Somorjai, Structural reanalysis of the rh(111)+($\sqrt{3} \times \sqrt{3}$) r30°-co and rh(111)+(2× 2)-3co phases using automated tensor leed, Surf. Sci. 391 (1–3) (1997) 176–182.

[11] A. Beutler, E. Lundgren, R. Nyholm, J.N. Andersen, B. Setlik, D. Heskett, On the adsorption sites for co on the rh(111) single crystal surface, Surf. Sci. 371 (2–3) (1997) 381–389.

[12] M.V. Ganduglia-Pirovano, M. Scheffler, Structural and electronic properties of chemisorbed oxygen on rh(111), Phys. Rev. B 59 (23) (1999) 15533.

[13] J. Gustafson, R.H. Westerström, O. Balmes, A. Resta, R. van Rijn, X. Torrelles, C. T. Herbschleb, J.W.M. Freken, E. Lundgren, Catalytic activity of the rh surface oxide: co oxidation over rh(111) under realistic condition, J. Phys. Chem. C 114 (2010) 4580–4583.

[14] F. Garcia-Martinez, F. Schiller, S. Blomberg, M. Shipilin, L.R. Merte, J. Gustafson, E. Lundgren, J.E. Ortega, Co chemisorption on vicinal rh(111) surfaces studied with a curved crystal, The Journal of Physical Chemistry C 124 (17) (2020) 9305–9313, https://doi.org/10.1021/acs.jpcc.0c00039.

[15] M.E. Turano, R.G. Farber, G. Hildebrandt, D.R. Killelea, Temperature dependence of co oxidation on rh (111) by adsorbed oxygen, Surf Sci 695 (2020) 121573, https://doi.org/10.1016/j.susc.2020.121573.

[16] C. Zhang, E. Lundgren, P.-A. Carlsson, O. Balmes, A. Hellman, L.R. Merte, M. Shipilin, W. Onderwaater, J. Gustafson, Faceting of rhodium(553) in realistic reaction mixtures of carbon monoxide and oxygen, J. Phys. Chem. C 119 (21) (2015) 11646–11652.

[17] L.A. DeLouise, E.J. White, N. Winograd, Characterization of co binding sites on rh111 and rh331 surfaces by xps and leed: comparison to eels results, Surf. Sci. 147 (1) (1984) 252–262, https://doi.org/10.1016/0039-6028(84)90179-1.

[18] J. Gustafson, M. Borg, A. Mikkelsen, S. Gorovikov, E. Lundgren, J.N. Andersen, Identification of step atoms by high resolution core level spectroscopy, Phys. Rev. Lett. 91 (5) (2003) 056102.

[19] A. Stroppa, F. Mittendorfer, J.N. Andersen, G. Parteder, F. Allegretti, S. Surnev, F. P. Netzer, Adsorption and dissociation of co on bare and ni-decorated stepped rh (553) surfaces, J. Phys. Chem. C 113 (3) (2008) 942–949.

[20] H.P. Koch, P. Singnurkar, R. Schennach, A. Stroppa, F. Mittendorfer, A rairs, tpd, and dft study of carbon monoxide adsorption on stepped rh(553), J. Phys. Chem. C 112 (3) (2008) 806–812.

[21] X.F. Ma, H.Y. Su, H.Q. Deng, W.X. Li, Carbon monoxide adsorption and dissociation on mn-decorated rh(111) and rh(553) surfaces: a first-principles study, Catal. Today 160 (2011) 228–233.

[22] S. Schwegmann, H. Over, V. De Renzi, G. Ertl, The atomic geometry of the o and co +o phases on rh(111), Surf. Sci. 375 (1996) 91–106.

[23] P.A. Thiel, E.D. Williams, J.T. Yates, W.H. Weinberg, The chemisorption of co on rh (111), Surf. Sci. 84 (1) (1979) 54–64.

[24] M.V. Ganduglia-Pirovano, M. Scheffler, A. Baraldi, S. Lizzit, G. Comelli, G. Paolucci, R. Rosei, Oxygen-induced rh 3 $d_{5/2}$ surface core-level shifts on rh (111), Phys. Rev. B 63 (20) (2001) 205415.

[25] A. Beutler, E. Lundgren, R. Nyholm, J.N. Andersen, B.J. Setlik, D. Heskett, Coverage- and temperature-dependent site occupancy of carbon monoxide on rh (111) studied by high-resolution core-level photoemission, Surf. Sci. 396 (1–3) (1998) 117–136.

[26] A.J. Medford, A. Vojvodic, J.S. Hummelshøj, J. Voss, F. Abild-Pedersen, F. Studt, T. Bligaard, A. Nilsson, J.K. Nørskov, From the sabatier principle to a predictive theory of transition-metal heterogeneous catalysis, J. Catal. 328 (2015) 36–42, https://doi.org/10.1016/j.jcat.2014.12.033.Special Issue: The Impact of Haldor Topsøe on Catalysis

[27] R. Nyholm, J.N. Andersen, U. Johansson, B.N. Jensen, I. Lindau, Beamline i311 at max-lab: a vuv/soft x-ray undulator beamline for high resolution electron spectroscopy, Nucl. Instrum. Methods. Phys. Res. A 467–468 (1) (2001) 520–524.

[28] G. Kresse, J. Hafner, Ab initio molecular dynamics for liquid metals, Phys. Rev. B 47 (1993) 558–561.

[29] G. Kresse, J. Hafner, Ab initio molecular-dynamics simulation of the liquid-metal-amorphous-semiconductor transition in germanium, Phys. Rev. B 49 (1994) 14251–14269.

[30] G. Kresse, D. Joubert, From ultrasoft pseudopotentials to the projector augmented-wave method, Phys. Rev. B 59 (1999) 1758–1775.

[31] P.E. Blöchl, Projector augmented-wave method, Phys. Rev. B 50 (1994) 17953–17979.

[32] J.P. Perdew, K. Burke, M. Ernzerhof, Generalized gradient approximation made simple, Phys. Rev. Lett. 77 (18) (1996) 3865–3868, https://doi.org/10.1103/PhysRevLett.77.3865.

[33] G. Henkelman, B.P. Uberuaga, H. Jónsson, A climbing image nudged elastic band method for finding saddle points and minimum energy paths, J. Chem. Phys. 113 (22) (2000) 9901–9904, https://doi.org/10.1063/1.1329672.

[34] M. Leetmaa, N.V. Skorodumova, Kmclib: a general framework for lattice kinetic monte carlo (kmc) simulations, Comput. Phys. Commun. 185 (9) (2014) 2340–2349, https://doi.org/10.1016/j.cpc.2014.04.017.

[35] M. Leetmaa, N.V. Skorodumova, Kmclib 1.1: extended random number support and technical updates to the kmclib general framework for kinetic monte-carlo simulations, Comput. Phys. Commun. 196 (2015) 611–613, https://doi.org/10.1016/j.cpc.2015.06.016.

[36] E. Lundgren, X. Torrelles, J. Alvarez, S. Ferrer, H. Over, A. Beutler, J.N. Andersen, Surface x-ray-diffraction study of the Rh(111) + (2 × 2) − 3CO structure, Phys. Rev. B 59 (1999) 5876–5880, https://doi.org/10.1103/PhysRevB.59.5876.

[37] P.J. Feibelman, B. Hammer, J.K. Nørskov, F. Wagner, M. Scheffler, R. Stumpf, R. Watwe, J. Dumesic, The co/pt(111) puzzle, J. Phys. Chem. B 105 (2001) 4018–4025, https://doi.org/10.1021/jp002302t.

[38] L. Köhler, G. Kresse, Density functional study of co on rh(111), Phys. Rev. B 70 (2004) 165405, https://doi.org/10.1103/PhysRevB.70.165405.

[39] A. Szabó, M.A. Henderson, J.T. Yates, Oxidation of co by oxygen on a stepped platinum surface: identification of the reaction site, J Chem Phys 96 (8) (1992) 6191–6202, https://doi.org/10.1063/1.462636.

[40] J. Xu, J.T. Yates, Catalytic oxidation of co on pt(335): a study of the active site, J Chem Phys 99 (1) (1993) 725–732, https://doi.org/10.1063/1.465745.

[41] J.T. Yates, Surface chemistry at metallic step defect sites, J. Vac. Sci. Technol., A 13 (3) (1995) 1359–1367, https://doi.org/10.1116/1.579564.

[42] R. Kose, D.A. King, Energetics and co-induced lifting of a (1 × 2) surface reconstruction of pt311, Chem Phys Lett 313 (1) (1999) 1–6, https://doi.org/10.1016/S0009-2614(99)01019-2.

[43] S. Blomberg, J. Zetterberg, J.F. Zhou, L.R. Merte, J. Gustafson, M. Shipilin, A. Trinchero, L.A. Miccio, A. Magaña, M. Ilyn, Strain dependent light-off temperature in catalysis revealed by planar laser-induced fluorescence, ACS Catal 7 (1) (2016) 110–114.

[44] J. Neugebohren, D. Borodin, H.W. Hahn, J. Altschäffel, A. Kandratsenka, D. J. Auerbach, C.T. Campbell, D. Schwarzer, D.J. Harding, A.M. Wodtke, et al., Velocity-resolved kinetics of site-specific carbon monoxide oxidation on platinum surfaces, Nature 558 (7709) (2018) 280–283, https://doi.org/10.1038/s41586-018-0188-x.

[45] G.B. Park, T.N. Kitsopoulos, D. Borodin, K. Golibrzuch, J. Neugebohren, D. J. Auerbach, C.T. Campbell, A.M. Wodtke, The kinetics of elementary thermal reactions in heterogeneous catalysis, Nat Rev Chem 3 (12) (2019) 723–732, https://doi.org/10.1038/s41570-019-0138-7.